Anti-phosphorylated histone H3 expression in Barrett's esophagus, low-grade dysplasia, high-grade dysplasia, and adenocarcinoma

Mahmoud Goodarzi[1], Arlene M Correa[2], Jaffer A Ajani[3], Stephen G Swisher[2], Wayne L Hofstetter[2], Sushovan Guha[4], Michael T Deavers[1], Asif Rashid[1] and Dipen M Maru[1]

[1]*Department of Pathology, The University of Texas MD Anderson Cancer Center, Houston, TX, USA;* [2]*Department of Thoracic and Cardiovascular Surgery, The University of Texas MD Anderson Cancer Center, Houston, TX, USA;* [3]*Department of Gastrointestinal Medical Oncology, The University of Texas MD Anderson Cancer Center, Houston, TX, USA and* [4]*Department of Gastroenterology, Hepatology and Nutrition, The University of Texas MD Anderson Cancer Center, Houston, TX, USA*

The high interobserver variability in grading dysplasia in Barrett's esophagus demands a biomarker that can be applied in routine surgical pathology practice. Immunohistochemistry for phosphorylated histone H3 is a reliable marker of identifying mitotic figures and has not been evaluated in Barrett's esophagus-associated neoplastic lesions. We retrospectively studied the expression of phosphorylated histone H3 in 88 endoscopic biopsy samples of Barrett's esophagus without dysplasia ($n = 19$), indefinite for dysplasia ($n = 11$), low-grade dysplasia ($n = 27$), high-grade dysplasia ($n = 19$), or adenocarcinoma ($n = 12$) from a sample of 54 patients. The samples were included after consensus diagnosis of two gastrointestinal pathologists on the hematoxylin–eosin (HE)-stained sections. Anti-phosphorylated histone H3-labeled mitotic figures were counted per 10 consecutive high-power fields (HPFs) in three distinct regions: surface epithelium, upper 2/3, and lower 1/3 of the crypts. Anti-phosphorylated histone H3-labeled mitotic counts for the three compartments of the crypts and the total scores for Barrett's esophagus, indefinite for dysplasia, low-grade dysplasia, high-grade dysplasia, and adenocarcinoma were compared using the Mann–Whitney U test. For each compartment, the number of anti-phosphorylated histone H3-positive nuclei was higher in low-grade dysplasia than in Barrett's esophagus without dysplasia or indefinite for dysplasia ($P < 0.001$), but no difference was found between Barrett's esophagus without dysplasia and indefinite for dysplasia. High-grade dysplasia biopsies had significantly more anti-phosphorylated histone H3-labeled mitotic figures in the surface epithelium than the low-grade dysplasia ($P < 0.001$). Adenocarcinoma had higher anti-phosphorylated histone H3-labeled mitotic figures than the high-grade dysplasia ($P < 0.001$). Our data support the previous findings of expansion of the proliferative zone and importance of surface mitotic figure in the progression of Barrett's esophagus—low-grade dysplasia–high-grade dysplasia. In addition, phosphorylated histone H3 is a potential supportive marker to histology in differentiating low-grade dysplasia from indefinite for dysplasia and high-grade dysplasia from adenocarcinoma in the mucosal biopsy samples.

Histological examination is considered the gold standard for assessing the risk for esophageal

Correspondence: Dr DM Maru, MD, Department of Pathology and Laboratory Medicine, Unit 085, The University of Texas MD Anderson Cancer Center, 1515 Holcombe Boulevard, Houston, TX 77030, USA.
E-mail: dmaru@mdanderson.org

adenocarcinoma in patients with Barrett's esophagus.[1] However, there is a high interobserver variability in the histological grading of Barrett's esophagus-associated dysplasia.[2–4] This variation is highest between low-grade dysplasia and indefinite for dysplasia and between high-grade dysplasia and early invasive adenocarcinoma.[3] Testing for aneuploidy, tetraploidy, and *p16* and *p53* genetic abnormalities, such as the loss of heterozygosity of chromosomes 9p and 17p,[5–7] have been shown to correlate with the risk of adenocarcinoma, but this is

difficult to obtain in routine surgical pathology practice, particularly given the limited amount of tissue available in an endoscopic biopsy sample. Immunohistochemical markers, such as α-methyl coenzyme A racemase (AMACR), p53, caspase 3, and survivin, are promising as ancillary tests to facilitate the grading of dysplasia and to diagnose early adenocarcinoma in Barrett's esophagus.[8–10]

Increased cell division with an expanded proliferation zone is consistently observed in gastrointestinal epithelial dysplastic lesions such as inflammatory bowel disease-associated dysplasia[11] and gastric dysplasia.[12] In Barrett's esophagus, dysplastic lesions have elevated proliferation index on Ki67 immunohistochemical staining. Despite the significance of proliferation in precancerous lesions, the role of phosphorylated histone H3, a surrogate marker for mitotic figure, has not been reported in Barrett's esophagus-associated dysplasia and adenocarcinoma. Two points of histone H3 are part of the histone octamer forming the eukaryotic nucleosome core, which has a fundamental role in DNA packaging. The nucleosome plus linker DNA form the nuclear chromatin. Thus, covalent modifications of the histone H3 can profoundly affect chromatin. The acetylation of certain lysine residues of histone H3 leads to gene expression, and methylation of the histone H3 causes gene silencing. The phosphorylation of histone H3 leads to chromatin condensation and mitosis.[13]

Previous biochemical studies[14] have shown that, in mammalian cells, histone H3 is phosphorylated at Ser10 during prophase, reaches a maximum during metaphase, diminishes during anaphase, and is lost during telophase and in the post-mitotic cytokinetic state. Because histone H3 protein is maximally phosphorylated during metaphase, a site-specific antibody for the phosphorylated form of the amino terminus of histone H3 is considered a powerful marker for detecting a mitotic figure.

Phosphorylated histone H3 has been shown to facilitate the grading of meningioma[15,16] and vulvar intraepithelial neoplasms[17] and the differentiation of malignant melanoma from benign melanocytic lesions.

Given the utility of phosphorylated histone H3 as a surrogate marker of identifying mitotic figure in multiple neoplasms, and the importance of cell proliferation in Barrett's esophagus-associated neoplastic lesions, we sought to quantitate mitotic figures and evaluate the pattern of distribution of mitotic figures using phosphorylated histone H3 immunostaining in the tissue samples of Barrett's esophagus, dysplasia, and adenocarcinoma.

Materials and methods

Study Groups

We retrospectively searched the surgical pathology database of the Department of Pathology, The University of Texas MD Anderson Cancer Center, Houston, Texas, and identified endoscopic biopsies with a diagnosis of Barrett's esophagus without dysplasia, Barrett's esophagus with indefinite for dysplasia, Barrett's esophagus with low-grade dysplasia, Barrett's esophagus with high-grade dysplasia or adenocarcinoma from 2005 to 2008. Information on the patient's age, gender, the presence and extent of Barrett's esophagus on endoscopy, endoscopic ultrasound, and computed tomography scan staging of the adenocarcinoma, participation in chemoprevention trials, and previous esophageal or gastric surgery were derived by retrospective review of the patients' electronic medical records. The patients who had ultrashort segment Barrett's esophagus, who had received preoperative chemoradiation, who had undergone previous gastric or esophageal surgery, and who were on chemoprevention trials of Cox 2 inhibitors for esophageal or colon cancers were excluded from the study. The study was approved by the institutional review board with waiver of informed consent (Lab-04–979).

All hematoxylin–eosin (HE)-stained slides were reviewed by two gastrointestinal pathologists in a blinded manner and graded independently. The cases were included in the study after a consensus diagnosis was reached. In cases of discrepancy, the slides were reviewed by a third gastrointestinal pathologist and a consensus diagnosis was rendered. The grading of dysplasia was performed according to the guidelines recommended by the Dysplasia Morphology Study Group[18] into indefinite for dysplasia, low-grade dysplasia, high-grade dysplasia, and adenocarcinoma. All patients with adenocarcinoma on biopsy samples had invasive carcinoma on subsequent resection specimens. Lesions with appropriate orientation on HE sections, containing all three compartments (surface, upper 2/3, and lower 1/3) of the metaplastic crypts, were included. Biopsy samples from the squamocolumnar junction and those with erosion/ulceration or more than occasional intraepithelial neutrophils were excluded.

Immunohistochemical Analysis

For this study, formalin-fixed paraffin-embedded sections (5 μm thick) from biopsy samples were used for immunohistochemical analysis. The immunohistochemistry stain was performed using a Bond Max automated immunostainer (Leica Microsystems, Bannockburn, IL, USA) at the CLIA-certified immunohistochemistry laboratory of the Department of Pathology. The sections were stained with antibody to phosphorylated histone H3 (rabbit polyclonal antibody, 1:400 dilution; Millipore, CA, USA) after antigen retrieval was achieved by treating the slides with Tris-EDTA buffer for 20 min. The primary antibody was detected using polymer detection kit (Leica Microsystems, Bannockburn, IL, USA) that included post-primary antibody, polymer, hydrogen peroxide, 3, 3-diaminobenzidine (DAB), hematoxylin, and DAB enhancer. After antigen retrieval the slides were

incubated with the primary antibody for 15 min, post-primary antibody for 8 min, polymer for 8 min, hydrogen peroxide (for blocking endogenous peroxidase) for 3 min, and DAB for 10 min, followed by counterstaining with hematoxylin and DAB enhancer for 8 min each. The slides were washed with ionized distilled water after each step. The slides were then dehydrated with alcohol and mounted with permount. A lymph node or tonsil was used as a positive control. Negative controls were obtained using an identical staining procedure while substituting primary buffer for primary antibody.

The anti-phosphorylated histone H3-positive mitotic figures were counted in three distinct compartments of the crypts: surface epithelial layer, upper 2/3 without the surface layer, and lower 1/3 of the crypts. In each case, the total number of nuclei staining for phosphorylated histone H3 was counted using a $\times 40$ objective magnification over 10 consecutive high-power fields (HPFs), and the average was calculated for each compartment. The 10 consecutive HPFs for a biopsy specimen usually covered an average of five crypts for each compartment. Because a lower level of punctate and scattered nuclear staining may be observed during interphase (the premitotic phase of the cell cycle), samples with positive nuclear staining that did not show intense chromatin aggregation were excluded.

Statistical Analysis

Phosphorylated histone H3 staining for the three different compartments and total scores for Barrett's esophagus, indefinite for dysplasia, low-grade dysplasia, high-grade dysplasia, and adenocarcinoma were compared using the Mann–Whitney U test. To make all observations independent and to apply the nonparametric tests appropriately, for each of these comparisons, data were excluded from patients with both types of lesion being compared (ie, if a patient had both Barrett's esophagus and low-grade dysplasia in a sample, that patient's data would be used to compare Barrett's esophagus with indefinite for dysplasia, high-grade dysplasia, and adenocarcinoma but not with low-grade dysplasia). A cutoff value for total anti-phosphorylated histone H3-labeled mitotic counts was derived from an ROC curve prepared for comparison of total anti-phosphorylated histone H3-labeled mitotic counts between low-grade dysplasia and indefinite for dysplasia and between adenocarcinoma and high-grade dysplasia. Statistical significance was defined as $P < 0.05$. The power of the study was calculated using SamplePower 2.0 software. The statistical package used was SPSS 15.0 for Windows (SPSS Inc., Chicago, IL, USA).

Results

The patient population consisted of 48 men and 6 women, with an average age of 64 years (range, 26–84 years), from whom 88 endoscopic biopsy samples were analyzed. In all, 48 patients had long-segment Barrett's esophagus, and 6 patients had short-segment Barrett's esophagus. We analyzed 19 biopsy samples of Barrett's esophagus without dysplasia (Figure 1a), 11 with indefinite for dysplasia (Figure 1b), 27 with low-grade dysplasia (Figure 1c), 19 with high-grade dysplasia (Figure 2a), and 12 with adenocarcinoma (Figure 2b). Additional 15 biopsies were excluded because of technical problems such as the focus of dysplasia being too small or improper orientation of the biopsy.

The anti-phosphorylated histone H3 positive-staining mitotic counts in Barrett's esophagus, dysplasia, and adenocarcinoma are summarized in Table 1. The surface epithelium in Barrett's esophagus without dysplasia (Figure 1d) was essentially negative for mitotic figure by phosphorylated histone H3 immunostain in all samples except for one showing 1 mitotic figure per 10 HPF. At least 1 mitotic figure per 10 HPF was observed by phosphorylated histone H3 immunostain in the upper 2/3 and lower 1/3 of crypts in 84% of the samples of Barrett's esophagus without dysplasia. Two samples with indefinite for dysplasia showed 1 mitotic figure per 10 HPF by phosphorylated histone H3 immunostain at the surface. At least 1 mitotic figure per 10 HPF in the upper 2/3 and lower 1/3 of the crypts was observed by phosphorylated histone H3 immunostain in 80% of the biopsy samples with indefinite for dysplasia (Figure 1e). There was no significant difference between Barrett's esophagus without dysplasia and indefinite for dysplasia in anti-phosphorylated histone H3-positive mitotic counts in any compartment of the crypt or in the total counts. The immunostain for phosphorylated H3 showed at least 1 mitotic figure in the surface epithelium in all but 1 ($>90\%$) biopsy samples with low-grade dysplasia. All biopsy samples with low-grade dysplasia showed at least 1 mitotic figure per 10 HPF in the upper 2/3 and lower 1/3 of the crypts by phosphorylated histone H3 immunostain (Figure 1f). Anti-phosphorylated histone H3-positive mitotic counts in low-grade dysplasia were significantly higher in all compartments than were those in Barrett's esophagus without dysplasia ($P < 0.001$, study power 97%) and indefinite for dysplasia ($P < 0.002$, study power 91%). The ROC curve comparing total anti-phosphorylated histone H3-positive mitotic counts between low-grade dysplasia and indefinite for dysplasia (Figure 3a) showed a cutoff value of 2.5 with 85% sensitivity (85% of all the low-grade dysplasia samples would be diagnosed as low-grade dysplasia) and 1−specificity of 0 (0% indefinite for dysplasia samples will be incorrectly identified as low-grade dysplasia). In other words, low-grade dysplasia can be diagnosed with 85% sensitivity and 100% specificity if a biopsy has the total phosphorylated histone H3 mitotic count higher than 3 per 10 HPF and the differential diagnosis is indefinite for dysplasia on HE sections.
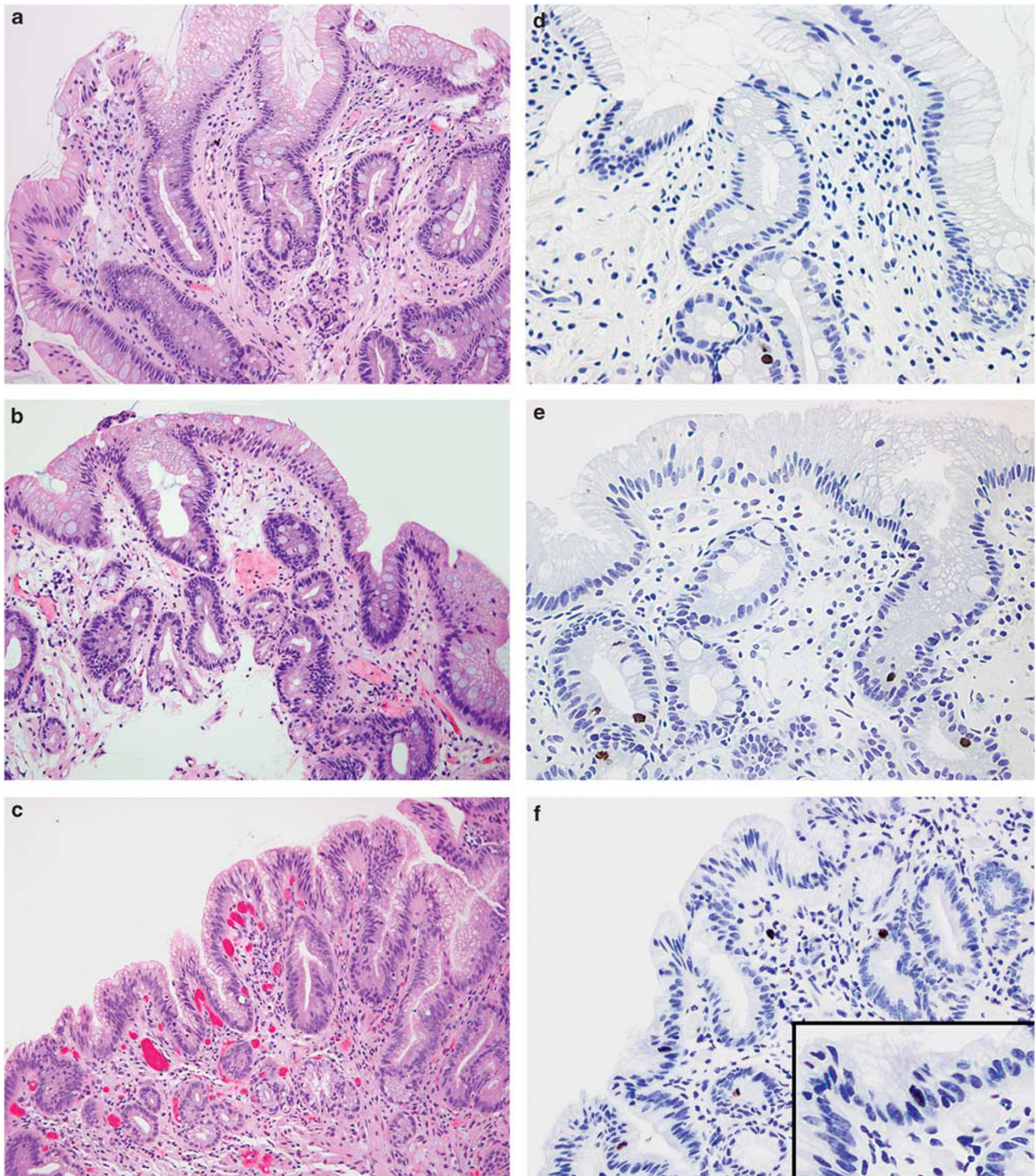
Figure 1 Hematoxylin–eosin-stained sections of Barrett's esophagus, (**a**), indefinite for dysplasia (**b**), and low-grade dysplasia (**c**), $\times 100$ magnification. Immunostain for phosphorylated histone H3 of Barrett's esophagus (**d**), indefinite for dysplasia (**e**), and low-grade dysplasia (**f**), $\times 200$ magnification. The immunostain for phosphorylated histone H3 shows anti-phosphorylated histone H3-positive nuclei in low-grade dysplasia with inset showing the presence of anti-phosphorylated histone H3-positive mitotic figure in the surface epithelium of low-grade dysplasia.

Mitotic figures were not identified on H&E sections in surface epithelium on scanning, low and intermediate power review in Barrett's esophagus without dysplasia, indefinite for dysplasia, and low-grade dysplasia. However, on meticulous review by HPF, only rare mitotic figures were observed on H&E sections in surface epithelium of a small number of biopsies with low-grade dysplasia and
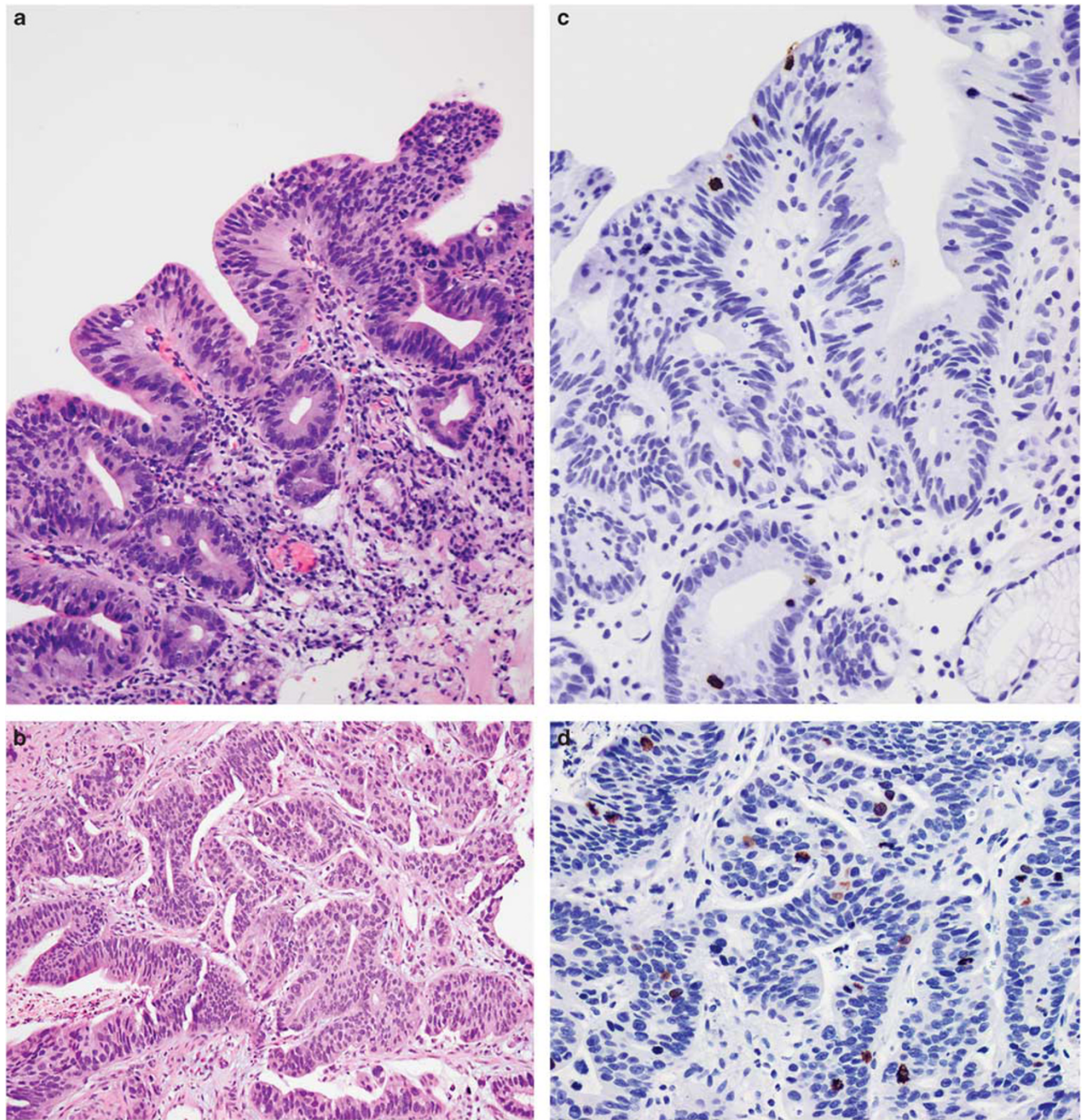
Figure 2 Hematoxylin–eosin sections of high-grade dysplasia (**a**) and adenocarcinoma (**b**), × 100 magnification. Immunostain for phosphorylated histone H3 of high-grade dysplasia (**c**) and adenocarcinoma (**d**), × 200 magnification. The immunostain for phosphorylated histone H3 shows higher anti-phosphorylated histone H3-positive cells in adenocarcinoma than in high-grade dysplasia.

none in Barrett's mucosa without dysplasia and indefinite for dysplasia. We observed mitotic figures on intermediate and high power on H&E sections in the upper 2/3 and lower 1/3 of crypts in low-grade dysplasia, indefinite for dysplasia, and Barrett's mucosa without dysplasia. Because of the stratification of the epithelium and cellular crowding in the upper 2/3 and lower 1/3 of the crypts, we could not achieve an accurate count for the mitotic figures on H&E section.

All biopsies with high-grade dysplasia showed ≥ 1 mitotic figures by phosphorylated histone H3 immunostain in the surface epithelium (Figure 2c). The anti-phosphorylated histone H3-positive mitotic counts in high-grade dysplasia were significantly higher in all compartments than were those in Barrett's esophagus without dysplasia ($P < 0.001$) and indefinite for dysplasia ($P < 0.001$). The anti-phosphorylated histone H3-positive mitotic count in the upper 2/3 and lower 1/3 of the crypts did not

Table 1 Comparison of mean ± s.d. pHH3 counts in different types of lesions and different compartments

Group (n)	Superficial	P-value	Upper 2/3	P-value	Lower 1/3	P-value	Total	P-value
BE (17)	0	NS	0.54 ± 0.36	NS	0.35 ± 0.35	NS	0.9 ± 0.58	NS
IND (10)	0.01 ± 0.03		0.59 ± 0.49		0.67 ± 0.56		1.27 ± 0.7	
BE (7)	0.01 ± 0.04	<0.001	0.48 ± 0.44	<0.001	0.12 ± 0.13	<0.001	0.62 ± 0.55	<0.001
LGD (15)	0.19 ± 0.11		2.36 ± 1.31		1.39 ± 0.83		3.95 ± 2.03	
BE (16)	0.01 ± 0.03	<0.001	0.50 ± 0.35	<0.001	0.3 ± 0.35	<0.001	0.81 ± 0.59	<0.001
HGD (16)	1.19 ± 0.80		2.58 ± 1.8		1.53 ± 0.82		5.29 ± 2.18	
BE (15)	—	—	—	—	—	—	0.98 ± 0.55	<0.001
ACA (11)							18.05 ± 4.43	
IND (11)	0.02 ± 0.06	<0.001	0.53 ± 0.50	<0.001	0.6 ± 0.57	<0.002	1.17 ± 0.73	<0.001
LGD (27)	0.19 ± 0.1		2.07 ± 1.22		1.56 ± 1.04		3.83 ± 1.84	
IND (11)	0.02 ± 0.06	<0.001	0.54 ± 0.50	<0.001	0.61 ± 0.56	0.01	1.17 ± 0.74	<0.001
HGD (19)	1.14 ± 0.78		2.41 ± 1.7		1.50 ± 0.97		5.06 ± 2.10	
IND (11)	—	—	—	—	—	—	1.17 ± 0.74	<0.001
ACA (12)							17.88 ± 4.26	
LGD (20)	0.2 ± 0.1	<0.001	1.62 ± 1.29	NS	1.83 ± 1.07	NS	4.26 ± 1.85	NS
HGD (12)	1.31 ± 0.47		2.01 ± 0.9		1.55 ± 0.85		4.89 ± 1.28	
LGD (27)	—	—	—	—	—	—	3.83 ± 1.84	0.001
ACA (12)							17.88 ± 4.26	
HGD (10)	—	—	—	—	—	—	4.94 ± 1.93	0.001
ACA (10)							16.66 ± 3.47	

ACA, adenocarcinoma; BE, Barrett's esophagus; HGD, high-grade dysplasia; IND, indefinite for dysplasia; LGD, low-grade dysplasia; NS, not significant; s.d., standard deviation.
Data were compared using the Mann–Whitney *U* test. Data were excluded from patients with both types of lesion being compared (ie, if a patient had both BE and LGD in a sample, that patient's data would be used to compare BE with IND, HGD, and ACA but not with LGD).
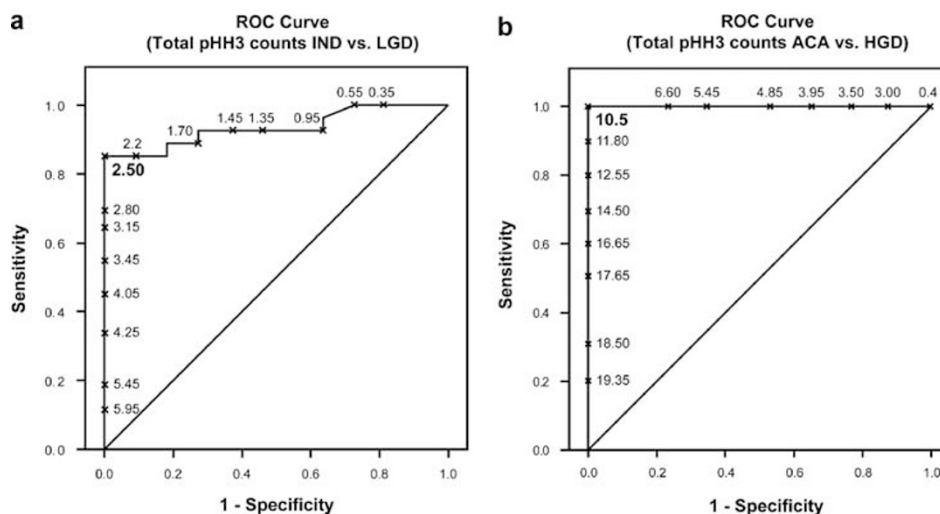

Figure 3 ROC curve comparing low-grade dysplasia (LGD) and indefinite for dysplasia (IND) (**a**) and (**b**) comparing adenocarcinoma (EAC) and high-grade dysplasia (HGD) with cutoff anti-phosphorylated histone H3 (pHH3)-positive mitotic counts at different sensitivity and 1−specificity values.

differ significantly between low-grade dysplasia and high-grade dysplasia. However, the anti-phosphorylated histone H3-positive mitotic count in the surface epithelium was significantly higher in high-grade dysplasia than in low-grade dysplasia ($P<0.001$, study power 90%). The anti-phosphorylated histone H3-positive mitotic counts in invasive adenocarcinoma (Figure 2d) were >1 per HPF
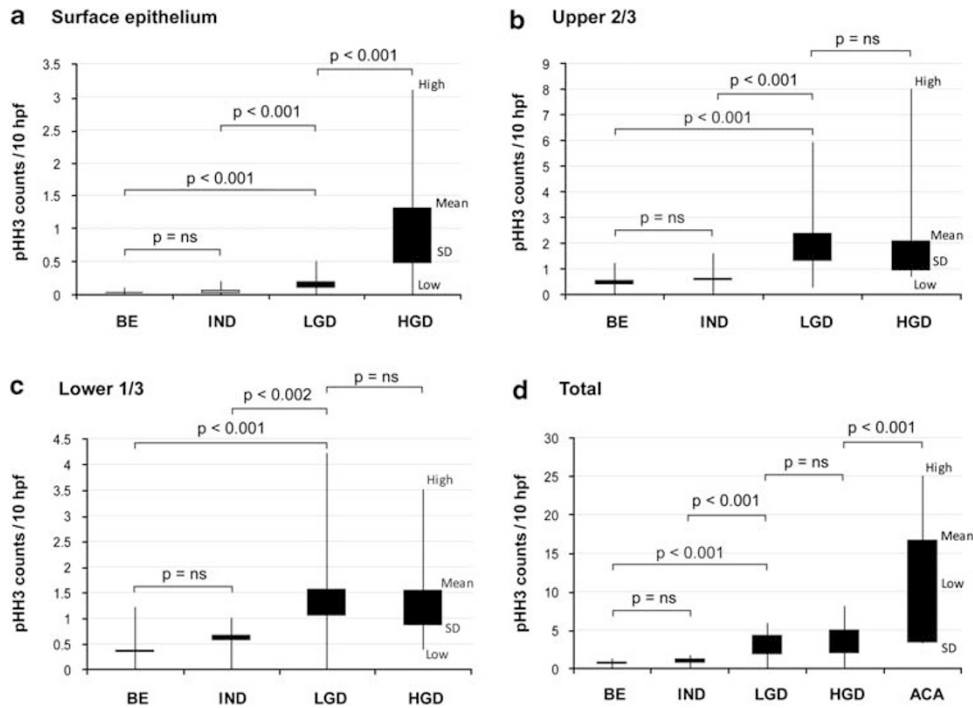
Anti-phosphorylated histone H3 staining in Barrett's esophagus
1618
M Goodarzi *et al*

Figure 4 Chart illustrating differences in the median, s.d., and range of anti-phosphorylated histone H3-positive mitotic counts in different compartments and total counts per 10 HPF in Barrett's esophagus (BE), indefinite for dysplasia (IND), low-grade dysplasia (LGD), high-grade dysplasia (HGD), and adenocarcinoma (EAC).

and were significantly higher than total anti-phosphorylated histone H3-positive mitotic counts in high-grade dysplasia ($P = 0.001$, study power 90%), low-grade dysplasia LGD ($P = 0.001$), indefinite for dysplasia ($P < 0.001$), and Barrett's esophagus without dysplasia ($P < 0.001$). The ROC curve comparing total anti-phosphorylated histone H3 mitotic counts between adenocarcinoma and high-grade dysplasia (Figure 4a) showed a cutoff value of 10.5 with 100% sensitivity (100% of all the adenocarcinoma samples would be diagnosed as adenocarcinoma as such) and 1−specificity of 0 (0% high-grade dysplasia samples will be incorrectly identified as adenocarcinoma). In other words, anti-phosphorylated histone H3-positive mitotic counts greater than 11 per 10 HPF (more than 1 per HPF) is diagnostic of adenocarcinoma, when the differential diagnosis is high-grade dysplasia on HE sections. We observed the presence of mitotic figures in the lower 1/3 of crypts in high-grade dysplasia and invasive component of adenocarcinoma on intermediate power. However, the surface mitotic figures were infrequent on H&E sections in the high-grade dysplasia and were observed only after meticulous search.

Figure 3 shows the range, median, and s.d. of total anti-phosphorylated histone H3-positive mitotic counts and anti-phosphorylated histone H3-positive mitotic counts in different crypt compartments in different lesions, thus illustrating the differences described above.

Discussion

To our knowledge, this study is the first to show that phosphorylated histone H3 is diagnostically useful for studying mitotic figures and alterations in proliferation compartments of different categories of Barrett's esophagus-associated neoplastic lesions. Higher surface anti-phosphorylated histone H3-positive mitotic counts in dysplastic lesions than in nondysplastic Barrett's esophagus indicates an expansion of the proliferation zone in dysplastic lesions. This finding, along with higher anti-phosphorylated histone H3-positive mitotic counts in other compartments in low-grade dysplasia than in indefinite for dysplasia, suggests the utility of phosphorylated histone H3 as an adjuvant marker to histology for differentiating between these two types of lesion. The ROC curve showed that average total pHH3 counts higher than 2.5 per 10 HPF have very high specificity in excluding any false-positive indefinite for dysplasia from low-grade dysplasia. On subgroup analysis, comparison of anti-phosphorylated histone H3 mitotic counts between cases with agreement and disagreement between two pathologists for indefinite for dysplasia and low-grade dysplasia did not yield conclusive results because of the smaller sample size for the subgroup in each lesion.

In our study, all the biopsies were appropriately oriented and samples from the squamocolumnar junction were excluded. These criteria reduced

interobserver variability in diagnosing indefinite for dysplasia, and thus the spectrum of biopsies with indefinite for dysplasia was somewhat limited. In addition, we excluded cases of indefinite for dysplasia or dysplasia with intraepithelial neutrophils to minimize the effects of oxygen-derived free radicals on mitotic activity. It would be interesting to compare phosphorylated histone H3 counts in similar grades of dysplasia, with and without the presence of intraepithelial neutrophils.

A number of markers have been explored that might be useful for differentiating dysplastic lesions in Barrett's esophagus. AMACR has been shown to be useful in differentiating between nondysplastic and dysplastic Barrett's esophagus. Dorer and Odze[8] showed that AMACR staining was absent in all biopsy samples of Barrett's esophagus without dysplasia but was positive in 38% of low-grade dysplasia samples, 81% of high-grade dysplasia samples, and 72% of adenocarcinoma samples. That study also found AMACR staining in 21% of samples that were originally diagnosed as indefinite for dysplasia. These findings were supported by the results of a study from Scheil-Bertram *et al*.[19] However, a recent study by Shi *et al*[20] showed AMACR expression at the rates of 12% in Barrett's esophagus without dysplasia, 47% in indefinite for dysplasia, 44% in low-grade dysplasia, 93% in high-grade dysplasia, and 96% in adenocarcinoma, suggesting that AMACR has lower specificity for distinguishing between Barrett's esophagus with and without dysplasia. The strength of AMACR is that the test is a simple qualitative assessment of positive cells. However, the pathogenic mechanism of AMACR expression in Barrett's esophagus-associated dysplastic lesions is unknown.

Parenti *et al*[10] showed overexpression of survivin, an inhibitor of programmed cell death, and of caspase 3, a protease that induces apoptosis, in both the proliferating and maturing compartments in dysplastic lesions compared with expression in Barrett's esophagus without dysplasia. However, no statistically significant difference in the expression of both markers was noted between low-grade dysplasia and high-grade dysplasia.

DNA ploidy has been shown to be an objective marker for the progression of Barrett's esophagus to dysplasia.[21] An aneuploid component in Barrett's esophagus is associated with the development of invasive adenocarcinoma.[22] However, flow-cytometric analysis requires extra tissue to obtain adequate cells for analysis, and another limiting factor is the lack of flow-cytometric equipment at smaller health care centers. Loss of heterozygosity of chromosome 17p has been determined to be a marker of Barrett's esophagus progression.[5] A *p53* mutation has been shown in the progression of Barrett's esophagus and is the underlying genetic change for loss of heterozygosity in chromosome 17p.[22] Tumor suppressor genes, such as *p16, RUNX3,* and *HPP1* that undergo methylation, have

been shown in one study[23] to function as biomarkers for predicting the progression of Barrett's esophagus to adenocarcinoma. Those investigators proposed a three-tiered risk-stratification system[24] based on three clinical parameters including histology, and four methylation-related parameters (normalized methylation values for *p16, HPP1,* and *RUN3* and methylation index). Although these markers hold promise as markers of progression, they need to be evaluated as adjuvant markers for the histological diagnosis of Barrett's esophagus-associated dysplasia. In contrast to some of these markers, the strength of phosphorylated histone H3 is its easy applicability to routine surgical pathology practice and its utility as a reliable validated marker of mitosis, which is a well-known feature of higher grade neoplastic lesions.

In mammalian cells, H3 phosphorylation at Ser-10 residue occurs throughout the condensing chromatin and is lost just before the formation of telophase chromosomes.[14] Furthermore, immunocytologic studies have shown that there is a precise spatial and temporal correlation between H3 phosphorylation and mitotic condensation.[23] Thus, pHH3 serves as a highly selective marker for direct quantitation of the mitotic index. Previous studies[9,25,26] using Ki-67 immunohistochemistry have shown expansion of the proliferation compartment in Barrett's esophagus with dysplasia. Hong *et al*[25] showed that Ki-67-positive nuclei in each mucosal compartment were significantly different in Barrett's esophagus without dysplasia than in Barrett's esophagus with low-grade dysplasia. However, they observed inconsistent results in indefinite for dysplasia samples. Olvera *et al*[26] found no value for Ki-67 immunohistochemical staining in distinguishing between low-grade dysplastic epithelium and cardiac mucosa or nondysplastic intestinal epithelium. Our study corroborates the results of the study by Hong *et al*,[25] except that we found lower mitotic counts in indefinite for dysplasia than in low-grade dysplasia. Ki-67 immunostain stains the cells in the G1, S, G2, and M phases of cell cycle,[27] whereas anti-phosphorylated histone H3 stains cells only in the M phase. Because different factors affect the different stages of the cell cycle, assessing cells only in the M phase is a more specific marker of cell division than is detecting cells in all phases of the cell cycle. In this respect, phosphorylated histone H3 is a better and specific marker for cell division than is Ki67. Because of this reason, we did not compare the Ki67 proliferative index with anti-phosphorylated histone H3 mitotic counts in this study.

A salient feature of our study was the showing of phosphorylated histone H3 as a marker of surface mitotic figures in Barrett's esophagus-associated dysplastic lesions. Immunostaining for phosphorylated histone H3 is a quick and reliable marker for identifying a mitotic figure.[28] Phosphorylated histone H3 is particularly useful in lesions in which mitotic figures on HE-stained sections are difficult

to count because of the paucity of mitosis, hypercellularity, cellular crowding, apoptosis, and admixed inflammatory cells. Because of these features; we faced difficulties in this study in counting mitotic figures on H&E sections in Barrett's esophagus and dysplasia, indicating that phosphohistone H3 is a more effective marker for identifying mitosis than mitotic counts performed on HE sections.

Our result of higher anti-phosphorylated histone H3-positive mitotic counts in the surface epithelium of high-grade dysplasia than in low-grade dysplasia is corroborated by results of another studies,[29,30] suggesting that surface mitotic figure is an important marker of a higher grade of dysplasia. In our study, mitotic figure was identified in each HPF by phosphorylated histone H3 immunostain in invasive adenocarcinoma and was threefold higher than high-grade dysplasia. In addition, an excellent ROC curve was obtained between adenocarcinoma and high-grade dysplasia, showing that a cutoff value for anti-phosphorylated histone H3-positive mitotic counts higher than 10.5 has 100% sensitivity and specificity in differentiating adenocarcinoma from high-grade dysplasia. These observations indicate that this marker holds promise as an ancillary marker for differentiating between early adenocarcinoma and high-grade dysplasia. This distinction is critical given recent advancements in endoscopic-based therapy in which the diagnosis of unequivocal invasion excludes patients from surveillance. Mitotic counts have shown to be useful in differentiating between *in situ* and invasive carcinoma in cervical squamous carcinoma,[31] endocervical adenocarcinoma,[32,33] and melanoma.[34] To our knowledge, this is the first study showing the utility of mitotic figures in differentiating invasive carcinoma from high-grade dysplasia in the Barrett's esophagus.

In summary, our data support those of previous studies that showed that the proliferation zone, from the base of the crypt to the surface epithelial layer, expands during the progression of dysplasia in Barrett's esophagus and that surface mitotic figure is an important marker in Barrett's esophagus-associated dysplastic lesions. In addition, our findings also indicate the potential use of phosphorylated histone H3 for differentiating low-grade dysplasia from indefinite for dysplasia and high-grade dysplasia from invasive adenocarcinoma in endoscopic biopsy samples; this potential warrants the further evaluation and validation of this marker in a larger and different subset of patients.

Acknowledgements

Disclosure/conflict of interest

The authors declare no conflict of interest.

References

1 Odze RD. Diagnosis and grading of dysplasia in Barrett's oesophagus. J Clin Pathol 2006;59:1029–1038.
2 Kerkhof M, van dekken H, Steyerberg EW, *et al.* Grading of dysplasia in Barrett's oesophagus: substantial interobserver variation between general and gastrointestinal pathologists. Histopathology 2007;50:920–927.
3 Montgomery E, Goldblum JR, Greenson JK, *et al.* Dysplasia as a predictive marker for invasive carcinoma in Barrett esophagus: a follow-up study based on 138 cases from a diagnostic variability study. Hum Pathol 2001;32:379–388.
4 Reid BJ, Haggitt RC, Rubin CE, *et al.* Observer variation in the diagnosis of dysplasia in Barrett's esophagus. Hum Pathol 1988;19:166–178.
5 Galipeau PC, Prevo LJ, Sanchez CA, *et al.* Clonal expansion and loss of heterozygosity at chromosomes 9p and 17p in premalignant esophageal (Barrett's) tissue. J Natl Cancer Inst 1999;91:2087–2095.
6 Kerkhof M, Steyerberg EW, Kusters JG. Aneuploidy and high expression of p53 and Ki67 is associated with neoplastic progression in Barrett esophagus. Cancer Biomark 2008;4:1–10.
7 Reid B, Levine DS, Longton G, *et al.* Predictors of progression to cancer in Barrett's esophagus: baseline histology and flow cytometry identify low and high-risk patient subsets. Am J Gastroenterol 2000;95:1669–1676.
8 Dorer R, Odze RD. AMACR immunostaining is useful in detecting dysplastic epithelium in Barrett's esophagus, ulcerative colitis, and Crohn's disease. Am J Surg Pathol 2006;30:871–877.
9 Lorinc E, Jakobsson B, Landberg G, *et al.* Ki67 and p53 immunohistochemistry reduces interobserver variation in assessment of Barrett's oesophagus. Histopathology 2005;46:642–648.
10 Parenti A, Leo G, Porzionato A, *et al.* Expression of survivin, p53, and caspase 3 in Barrett's esophagus carcinogenesis. Hum Pathol 2006;37:16–22.
11 Shinozaki M, Watanabe T, Kubota Y, *et al.* High proliferative activity is associated with dysplasia in ulcerative colitis. Dis Colon Rectum 2000;43:S34–S39.
12 Miracco C, Spina D, Vindigni C, *et al.* Cell proliferation patterns and p53 expression in gastric dysplasia. Int J Cancer 1995;62:149–154.
13 Alberts B, Johnson A, Lewis J, *et al.* Molecular Biology of the Cell. Garland Science: New York, pp 213–215 (Chapter 4).
14 Hendzel MJ, Wei Y, Mancini MA. Mitosis-specific phosphorylation of histone H3 initiates primarily within pericentromeric heterochromatin during G2 and spreads in an ordered fashion coincident with mitotic chromosome condensation. Chromosoma 1997;106:348–360.
15 Kim YJ, Ketter R, Steudel WI, *et al.* Prognostic significance of the mitotic index using the mitosis marker anti-phosphohistone H3 in meningiomas. Am J Clin Pathol 2007;128:118–125.

16 Ribalta T, McCutcheon IE, Aldape KD, *et al.* The mitosis-specific antibody anti-phosphohistone-H3 facilitates rapid reliable grading of meningiomas according to WHO 2000 criteria. Am J Surg Pathol 2004; 28:1532–1536.

17 Davidson EJ, Morris LS, Scott IS, *et al.* Minichromosome maintenance (Mcm) proteins, cyclin B1 and D1, phosphohistone H3 and *in situ* DNA replication for functional analysis of vulvar intraepithelial neoplasia. Br J Cancer 2003;88:257–262.

18 Riddell RH, Goldman H, Ransohoff DF, *et al.* Dysplasia in inflammatory bowel disease: standardized classification with provisional clinical applications. Hum Pathol 1983;14:931–968.

19 Scheil-Bertram S, Lorenz D, Ell C, *et al.* Expression of alpha-methylacyl coenzyme A racemase in the dysplasia carcinoma sequence associated with Barrett's esophagus. Mod Pathol 2008;21:961–967.

20 Shi XY, Bhagwandeen B, Leong AS. p16, cyclin D1, Ki-67, and AMACR as markers for dysplasia in Barrett esophagus. Appl Immunohistochem Mol Morphol 2008;16:447–452.

21 Reid BJ, Blount PL, Rubin CE, *et al.* Flow-cytometric and histological progression to malignancy in Barrett's esophagus: prospective endoscopic surveillance of a cohort. Gastroenterology 1992;102: 1212–1219.

22 Reid BJ, Prevo LJ, Galipeau PC, *et al.* Predictors of progression in Barrett's esophagus II: baseline 17p (p53) loss of heterozygosity identifies a patient subset at increased risk for neoplastic progression. Am J Gastroenterol 2001;96:2839–2848.

23 Sato F, Jin Z, Schulmann K, *et al.* Three-tiered risk stratification model to predict progression in Barrett's esophagus using epigenetic and clinical features. PLoS ONE 2008;3:e1890.

24 Hendzel MJ, Nishioka WK, Raymond Y, *et al.* Chromatin condensation is not associated with apoptosis. J Biol Chem 1998;273:24470–24478.

25 Hong MK, Laskin WB, Herman BE, *et al.* Expansion of the Ki-67 proliferative compartment correlates with degree of dysplasia in Barrett's esophagus. Cancer 1995;75:423–429.

26 Olvera M, Wickramasinghe K, Brynes R, *et al.* Ki67 expression in different epithelial types in columnar lined oesophagus indicates varying levels of expanded and aberrant proliferative patterns. Histopathology 2005;47:132–140.

27 Gerdes J, Lemke H, Baisch H, *et al.* Cell cycle analysis of a cell proliferation-associated human nuclear antigen defined by the monoclonal antibody Ki-67. J Immunol 1984;133:1710–1715.

28 Baehner R, Weidner N. Enhanced mitotic figure counting in breast carcinomas using a mitosis-specific antibody: anti-phosphohistone-H3 (PHH3). Mod Pathol 2000;13:17A.

29 Coco D, Srivastava A, Sanchez C, *et al.* Surface mitoses are a predictor of cancer progression in Barrett's esophagus. Lab Invest 2009;89:127A.

30 Sirieix P, O'Donovan M, Brown J, *et al.* Surface expression of minichrome maintenance protein provides a novel method for detecting patients at risk for developing adenocarcinoma in Barrett's esophagus. Clin Cancer Res 2003;9:2560–2566.

31 Al-Nafussi AI, Hughes DE. Histological features of CIN 3 and their value in predicting invasive microinvasive squamous carcinoma. J Clin Pathol 1994;47:799–804.

32 Moritani S, Ioffe OB, Sagae S, *et al.* Mitotic activity and apoptosis in endocervical glandular lesions. Int J Gynecol Pathol 2002;21:125–133.

33 Witkiewicz A, Lee KR, Brodsky G, *et al.* Superficial (early) endocervical adenocarcinoma *in situ*: a study of 12 cases and comparison to conventional AIS. Am J Surg Pathol 2005;29:1609–1614.

34 Nasr MR, El-Zammar O. Comparison of pHH3, Ki-67, and survivin immunoreactivity in benign and malignant melanocytic lesions. Am J Dermatopathol 2008;30:117–122.